CIÊNCIA E TECNOLOGIA

CORRELATION BETWEEN VEGETATION INDICES OBTAINED BY RPA AND GRAIN YIELD

HELTON APARECIDO ROSA[1], JERRY ADRIANI JOHANN[2], WILLYAN RONALDO BECKER[2], JOÃO FELIPE CESAR SILVEIRA[2], IDELVAN BONADIMAN BLANCO[2]

[1]Centro Universitário Assis Gurgacz - FAG
[2]Universidade Estadual do Oeste do Paraná - UNIOESTE
<helton.rosa@hotmail.com>, <jerry.johann@hotmail.com>, <willyan.becker@outlook.com>, <joaofelipecs17@gmail.com>, <idelvanblanco@gmail.com>
DOI: 10.21439/conexoes.v18i0.3335

Resumo. The objective of this study was to evaluate the correlations between vegetation indices (VI), obtained by RGB camera on flights of *Remotely piloted aircraft System* (RPA), with yield maps of agricultural crops. Monitoring was carried out during 4 harvest seasons: soybean 2018/19, maize (2019), soybean 2019/20 and wheat (2020), in two areas of a rural property located in Toledo, Paraná. During the harvests, periodic flights were performed using DJI-branded RPA Phantom 3 Advanced. For the generation of orthomosaic, Agisoft PhotoScan software (*Free trial*) was used. After the RGB bands normalization, the vegetation indices MPRI, VARI, GLI and ExG were calculated for 3 flight dates in each harvest in the study areas. At the end of the crop cycle, samples were collected to create the yield maps. With the yield data, descriptive statistics analyzes were performed and, later, the correlation between the VIs and the yields of each harvest was performed using Spearman's correlation coefficient (r_s). According to the research, it would be suggested that the farmer carry out surveys with RPA with RGB camera in soybean crop, mainly in R7 stage, in maize at VT (bolting) stage and in wheat at tillering stage, since these phenological stages showed higher correlations and between the VIs and the yield of each crop. The pairs of VIs MPRI and VARI, GLI and ExG were similar as vegetative indicators, so only two of them would already have the capacity to represent the variations existing in the areas of the study between the dates.

Palavras-chave: drone; MPRI; VARI; EXG; GLI; remote sensing.

CORRELAÇÃO ENTRE ÍNDICES DE VEGETAÇÃO OBTIDOS POR RPA E PRODUTIVIDADE DE GRÃOS

Abstract. O objetivo deste estudo foi avaliar correlações entre índices de vegetação (IV), obtidos por câmera RGB em voos de *Remotely Piloted Aircraft System* (RPA), com mapas de produtividade de culturas agrícolas. O monitoramento foi realizado durante quatro safras agrícolas: soja 2018/19, milho (2019), soja 2019/20, trigo (2020), em duas áreas de propriedade rural localizadas no município de Toledo – Paraná. Durante as safras, foram realizados voos utilizando RPA Phantom 3 Advanced, da marca Dji. Para a geração dos ortomosaicos, utilizou-se *software* Agisoft PhotoScan. Após a normalização das bandas RGB, calcularam-se os índices de vegetação MPRI, VARI, GLI e ExG, para três datas de voos em cada safra. Na parte final do ciclo das culturas, realizou-se coleta de amostras para criação dos mapas de produtividade. Com os dados de produtividade, foram realizadas análises de estatística descritiva e, posteriormente, realizada a correlação entre os IVs e as produtividades de cada safra, por meio do coeficiente de correlação de Spearman (r_s). De acordo com a pesquisa, seria indicado que o produtor fizesse levantamentos com RPA com câmera RGB na cultura da soja, principalmente no estádio R7, no milho no estádio de VT (pendoamento) e no trigo no estádio de perfilhamento, visto terem sido esses os estádios fenológicos que apresentaram maiores correlações e entre os IVs e as produtividades de cada cultura. Os pares de IVs MPRI e VARI, GLI e ExG se mostraram semelhantes como indicadores vegetativos, portanto, somente dois deles já teriam capacidade de representar as variações existentes nas áreas do estudo entre as datas.

Keywords: drone; MPRI; VARI; EXG; GLI; sensoriamento remoto.

1 INTRODUCTION

The modernization that is taking place in several sectors, has also reached agriculture, in view of the fact that in recent years crop yield has increased, with computerization in the field. One of the factors responsible for this is the adherence of farmers to precision farming (PF) techniques, which provide important tools, that can be used to evaluate productive capacity and to assist decision making, aiming to achieve higher yield, with less environmental impact (Yuzugullu *et al*., 2020).

One of the sources of information for PF is data acquired through remote sensing (RS), which consists of obtaining spectral data related to the crops agronomic characteristics, without direct contact with the targets, with advantages of enabling data collection in less time and with reduced impacts (Costa; Nunes; Ampatzidis, 2020), providing information on the stage of the crop over the harvest at different scales (Weiss; Jacob; Duveiller, 2020).

Difficulties that once existed for acquiring satellite image data, especially those that require lower spatial resolution, because they are paid, can be solved by using *the Remotely Piloted Aircraft System* (RPA), which have great flexibility and the ability to provide many specific information about the area (Alexopoulos *et al*., 2023). Another advantage is the possibility of using commercial cameras, free of more complex and expensive sensors, allowing greater dissemination and reducing costs related to field operation (Andrade Junior *et al*., 2021; Freire-Silva *et al*., 2019).

Thus, the development of RPA provided a new approach to PF, enabling the acquisition of high-resolution space-temporal images (Zhou *et al*., 2020) and providing new tools for vegetation monitoring and data with very high temporal and spatial resolutions (Banerjee; Raval; Cullen, 2018).

One of the products generated by PF using RPA is the vegetation index (VI), which, according to Costa, Nunes e Ampatzidis (2020), represents a combination between two or more spectral bands, generated by mathematical equations, which have the objective of synthesizing and improving the relation of data with vegetation biophysical parameters.

These combinations faithfully represent variations in the leaves, not only in seasonal terms, but across the Earth's surface, with the objective of detecting variabilities, which could help in the study of the spectral and temporal patterns of crops during their phenological cycle. and in association with factors that condition the development of grains, contributing to farmers decision-making (Barbedo, 2019).

Many PF applications use vegetation indexes to measure plant phenological parameters (Semeraro *et al*., 2019). Some indices used in agriculture use RGB and infrared lengths such as: NDVI (Rouse *et al*., 1974) and SAVI (Huete, 1988). Other indices use only RGB, namely: VARI (Gitelson *et al*., 2003), MPRI (Yang; Willis; Mueller, 2008), GLI *Green Leaf Index* (Louhaichi; Borman; Johnson, 2001) and Excess of green - ExG (Woebbecke *et al*., 1995).

Analyzing 15 vegetation indices obtained with RPA equipped with multispectral camera, (Hoyos-Villegas; Fritschi, 2013) verified that indices using visible and infrared spectrum wavelengths, such as NDVI and SAVI, showed the ability to detect changes in biomass, canopy coverage and senescence, particularly in the grain filling stages.

Prestes *et al*. (2020) evaluated VIs that use only visible lengths and VIs that also use infrared lengths throughout soybean development and found that VARI presented the highest correlation with crop yield on the four dates evaluated, with values higher than NDVI. These results provide a good perspective on the use of the RGB camera that can provide a cost-effective and viable solution for estimating crop yield.

The objective of this study was to evaluate the correlations of the VIs MPRI, VARI, GLI and ExG, obtained by RGB camera on RPA flights, with crop yield data in four harvests (soybean 2018/2019, maize 2019, soybean 2019/2020 and wheat 2020), in rural property located in Toledo, Paraná State.

2 MATERIALS AND METHODS

2.1 Study area

Monitoring was carried out in two areas (37 hectares and 22 hectares) of a rural estate (Figure 1) located in the municipality of Toledo – Paraná. The soil of the region is classified as Dusky-red Latosol (EMBRAPA, 2018). The climate of the region is Cfa type, humid subtropical, with average temperatures of 21.1ºC, and average annual rainfall between 1550 and 1650 mm (Aparecido *et al*., 2016).

2.2 Flight planning with RPA

For monitoring the areas, an overflight was performed with the RPA Phantom 3 Advanced Model, type quadcopter multirotor type. RPA has an approximate mass of 1.3 kg, with a flight autonomy of approximately 23 min, in ideal climatic conditions (without wind), and equipped with an RGB camera with 12.4 megapixel resolution, coupled to a 3-axis stabilization gimbal with

Figure 1: Location of the experiment and sampling points of yield samples.

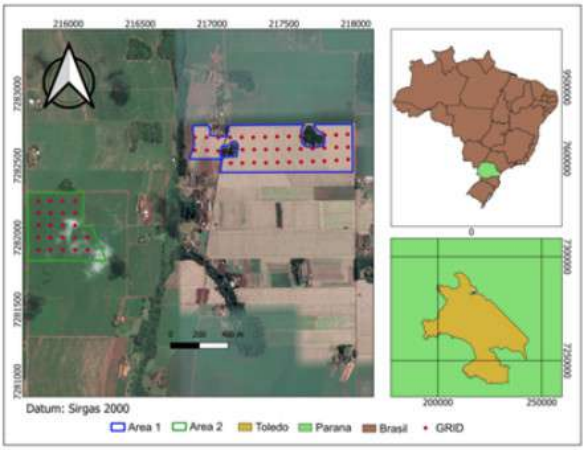

tilt angle control, ranging from 90º to +30º, allowing video recording at 2.7K and shutter speed of 1/8000 s.

During the experiment period, three flights were performed in each harvest, totaling over four harvests 24 flights (Table 1). It is worth pointing out that for maize harvest (2019), a flight date was discarded, because the generated orthomosaic presented failures.

The flight plans were carried out with the aid of Drone deploy software (*Free trial*), with an altitude of 120 m, generating a *Ground Sample Distance* (GSD) of, approximately, 5 cm/*pixel*. The vertical and horizontal overlaps established for the flights were 70%. Specific software Agisoft PhotoScan (*Free trial*) was used to generate the orthomosaic. For geometric correction of the areas and accuracy of the surveys, 15 fixed control points (CPs) were used in the areas (15 CPs in area 1 and 11 CPs in area 2); their geographic coordinates were obtained with the GNSS NAVCON receiver, tracking in phases L1/L2. Subsequently, correction was performed with IBGE data through Precise Point Positioning (PPP). After the images were processed and the orthomosaic generation, the R, G, B bands were separated, with the help of the "Divide RGB Bands" tool of QGIS (version 3.10). After this stage, the band normalization process was performed, aiming to correct possible imperfections, following methodologies performed by Ballesteros *et al*. (2018). The special resolution of the RPA images was transformed to 10 m using the resample command of QGIS, with the objective of standardizing *the pixel size* for the Sentinel-2 satellite pixel size, which is the same size.

2.3 Vegetation indices

After this normalization, the MPRI, VARI, GLI and ExG vegetation indices were calculated using the QGIS software for the three flight dates in the study areas (Table 2), using interval criteria for the classes classification.

2.4 Yield of agricultural crops

At the end of the crops cycle of each harvest, production samples collection was performed to elaborate the yield maps. The area collected was 1 m² per sample point (Figure 1), manually performed in a regular grid of one sample per hectare, 37 samples for area 1 and 22 samples for area 2.

After each harvest, the grain threshing of each sample was performed, using a grain threshing specific machine, and after weighing, grain moisture evaluation, in sequence, according to the seeds analysis rule (SAR), to be corrected to 13% of moisture (Brasil, 2009) and finally, obtain the weight of the grains, which were converted into kilograms per hectare (kg ha^{-1}).

2.5 Data analysis

The data interpolation was performed by the ordinary Kriging method, using the precision agriculture complement: *QGIS software Smart-Map*, for generating the yield maps used in the research. With the yield data, a descriptive statistical analysis was performed. The coefficients of variation (CVs) for each harvest were evaluated according to the classification of Gomes (2009): low (< 10%); medium (between 10 and 20%); high (between 20 and 30%); and very high (> 30%).

Subsequently, the Spearman correlation coefficient (r_s) was determined between the VIs and the yields of each harvest. It is worth pointing out that the Spearman coefficient (r_s) is used when the relationship between the data pairs is not linear or when there is no normality in the data set. Its result may vary between 1 and -1, where 1 means a perfect correlation, 0 means that there is no correlation, and -1 that there is a perfect negative correlation (Inman, 1994).

In order to determine the correlation between the yields of the areas collected in the field, the VIs were quantified in a *buffer* of 30 m radius around *the grid coordinate* presented in Figure 2D, with the objective of using subsequently the average of 25 pixels of this region for the analysis. This procedure was performed in the Quantum GIS software (QGIS, 2021), using *the Zonal Statistics function* that allows quantifying the VIs mean values in each sampling point.

Table 1: Period of flights carried out with RPA and the crops phenological stage during the four harvests

	Harvests/Flights	Flight 1		Flight 2		Flight 3	
		DAS	Stages	DAS	Stages	DAS	Stages
area 1	Soybean 2018/2019	48	R3	59	R5	80	R6
	Mayze 2019	30	V3	—	—	119	VT
	Soybean 2019/2020	48	R2	75	R4	82	R5
	Wheat 2020	42	PER	65	FL	92	EG
area 2	Soybean 2018/2019	60	R4	75	R6	94	R7
	Mayze 2019	44	V3	—	—	133	R1
	Soybean 2019/2020	47	R2	74	R3	81	R5
	Wheat 2020	42	PER	65	FL	92	EG

Subtitles: DAS = Days after sowing. **Soybean**: R2 = Full flowering; R3 = Beginning of pod formation; R4 = pod fully developed; R5 = Start of grain filling; R6 = Full or full grain; R7 = Start of maturation. **Mayze**: V3 = 3 Leaves developed; V7 = 7 developed leaves; VT = Bracing; R1 = Flowering and pollination. **Wheat**: PER = Tillering; FL= Flowering; EG = Grain filling.

Table 2: Vegetation indices obtained with RGB camera attached to RPA

Vegetation index	Equation
MPRI	$\frac{GREEN-RED}{GREEN+RED}$
VARI	$\frac{GREEN-RED}{GREEN+RED-BLUE}$
GLI	$\frac{GREEN-RED-BLUE}{GREEN+RED+BLUE}$
ExG	$(2.GREEN - RED - BLUE)$

Subtitles: RED = reflectance in the red region (nm); GREEN = reflectance in the green region; BLUE = reflectance in the blue region.

Correlations were determined in the Minitab software (MINITAB, 2003) and significant correlations were considered for those whose *p-value* was less than 5% significance (0.05). To evaluate the correlations, Callegari-Jacques (2003) classification was used, in which rs can be assessed qualitatively by the following intervals: $0.9 \leq \mid r_s \mid \leq 1.0$, meaning very strong correlation; $0.7 \leq \mid r_s \mid < 0.9$, meaning strong correlation; $0.4 \leq \mid r_s \mid \leq < 0.7$, meaning moderate correlation; $0.2 \leq \mid r_s \mid < 0.4$, meaning weak correlation; $0.0 \leq \mid r_s \mid < 0.2$, meaning very weak correlation.

3 RESULTS AND DISCUSSION

3.1 Vegetation indices of the harvests and areas

When analyzing the MPRI index along the harvests (Figure 2A), it is verified that the highest values were found for soybean (2019/2020), with 48 DAS, being in stage R3, in which the pod is under formation, has approximately 5 mm in length and presented a large part of the map with values between 0.30 and 0.50. For the other harvests, the tendency was, on the first flight date, to present lower values, as in the 2019 maize crop, which, on flight 30 DAS, showed bands with values between -0.30 and -0.10 in almost the whole map, because maize is at the beginning of development, in V3 stage, with only three developed leaves and a great part of the soil still exposed. Values in this range were also found in almost the whole map with 92 DAS for wheat harvest (2020). In this case, due to the culture being almost at the end of the cycle, approaching the maturation stage. For the same wheat harvest, at 42 DAS (tillering phase) in the northwest part of the map, regions with low MPRI values were also found, due to erosion caused by heavy rains that occurred a few days after the crop sowing, which resulted in runoff with soil loss, along with seeds that had not germinated yet.

For the VARI index, visual behavior similar to the MPRI index was observed, only with ranges of values included in a different scale, with higher values of the index, also found in soybean (2019-2020), with 48 DAS (between 0.60 and 1.00) (Figure 2B).

The GLI (Figure 2C) and ExG (Figure 2D) indices showed some behaviors different from that seen in the previous indices (MPRI and VARI), because there was no such large decrease for the VIs on the last flights performed; there was also emphasis in some parts, such as the south of the 65 DAS map in the wheat crop, which was flourishing and showed a range with values higher than the rest of the area for that date. A little less noticeable, but still possible to notice the erosion behavior in the northwest part of the wheat area in 42 DAS (tillering) and 65 DAS (flowering and fruiting).

In the case of MPRI for area 2 (Figure 3A), it was also verified that, in general, the highest values of the index were for soybean area 2019/2020, mainly at 47 DAS, in stage R2 (full flowering), with values between

Figure 2: Vegetation index for area 1, in the four harvests.

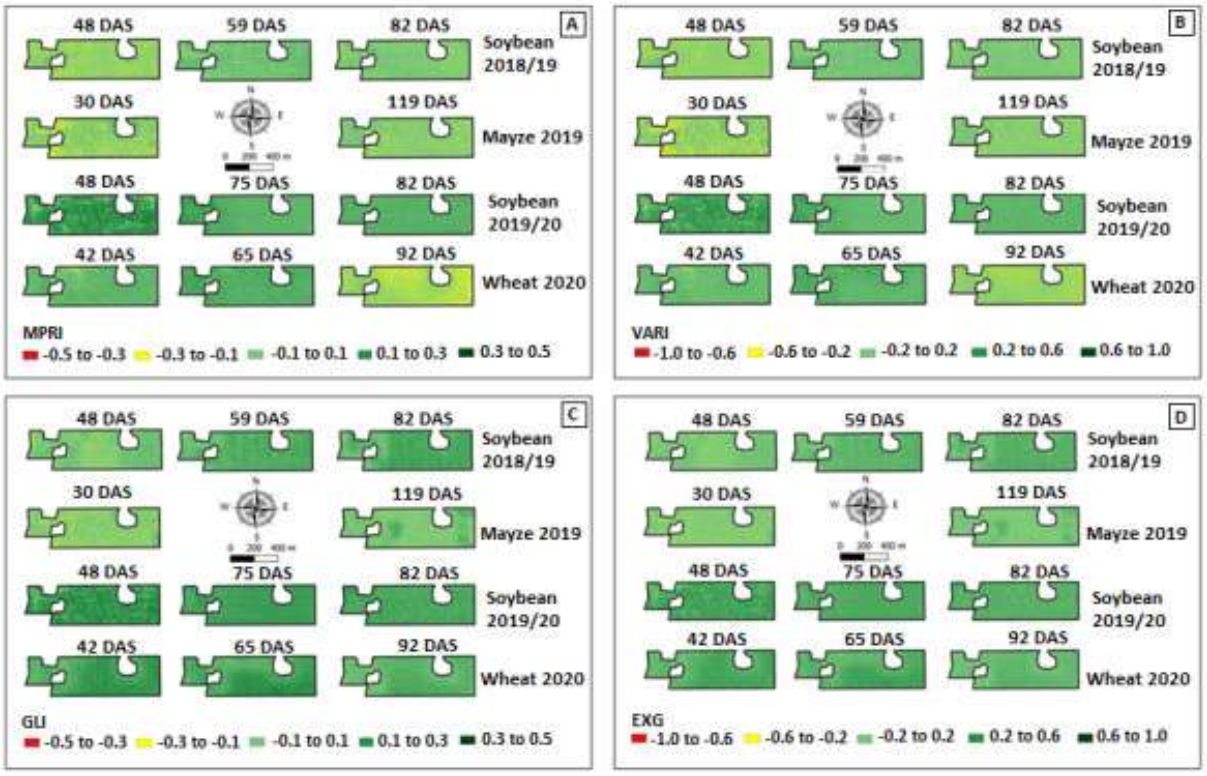

0.30 and 0.50. Except for this harvest, the remaining ones showed on the last flight a discrepancy in the values along the area, with bands showing values below the index (between -0.30 and -0.10). In 94 DAS (soybean 2018/2019), in R7, at the beginning of maturation, a range of values higher than the rest of the area was observed in the east part of the map, as well as in 133 DAS (maize 2019), with the crop in R1 (flowering and pollination). This difference occurred, as that range of area corresponding to approximately 2 ha represented part of the area that was sown with another variety in the soybean crop and had a different end of cycle than the rest, which resulted in a different sowing date also in the subsequent crop (maize 2019). VARI for area 2 presented visual behavior similar to MPRI, although with greater mildness (Figure 3B). Differences were also observed for 94 (soybean 2018/2019) and at 133 DAS for maize harvest (2019). At 47 DAS (R2) in the soybean 2019/2020 harvest, the values in most part of the map were between 0.60 and 1.00, the highest ones, when compared to the four harvests.

The GLI (Figure 3C) and ExG (Figure 3D) indices for area 2 also indicated that 47 DAS (Soybean 2019/2020) was the date on which the index expressed its highest values when compared all the harvests. Greater uniformity among the dates was found, except for maize with 133 DAS, in regions east and west of the map that presented lower values, when compared to the rest of the area. For wheat harvest (2020), with 65 DAS, the central portion of the map presented values higher than those found in the other regions of the area.

3.2 Harvests yield and areas

Based on the yield maps of area 1 (Figure 4), it is observed that, for the soybean 2018-2019 harvest, the highest values were concentrated in the region west of the thematic map, with values exceeding 3000 kg ha^{-1}, while in the central part of the map going east, the values were mostly between 2900 and 2980 kg ha^{-1}. For the maize 2019 harvest, a large region of the western center of the map presented higher yield values (above 6000 kg ha^{-1}), part more to the southeastern of the map obtaining lower yields (between 5550 and 5840 kg ha^{-1}).

For soybean 2019/2020 harvest, also the western region of the map presented the highest values, between

Figure 3: Vegetation index for area 2, in the four harvests.

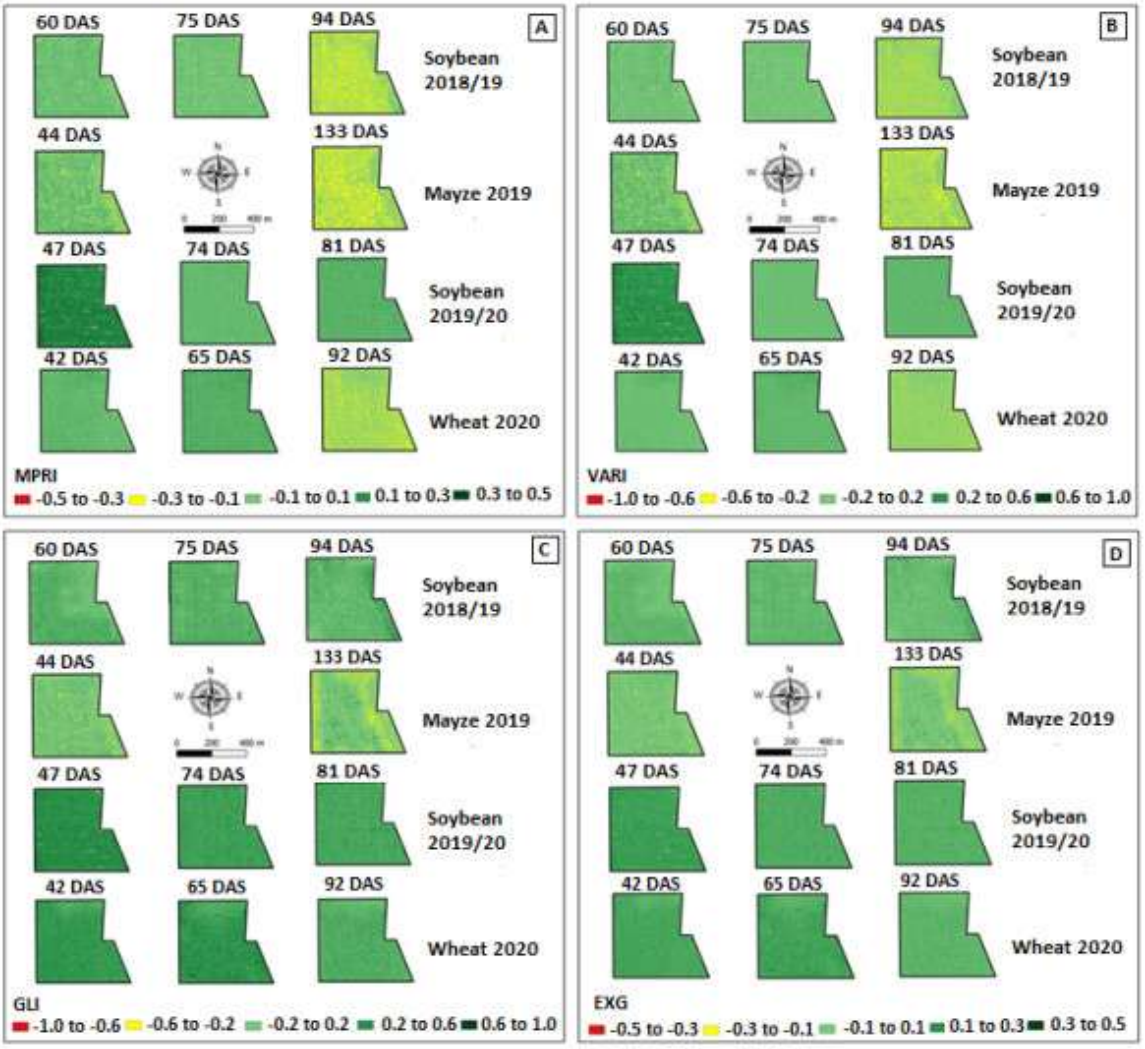

3960 and 4600 kg ha^{-1}. Lower yield values were concentrated in the south of the map (3000 to 3200 kg ha^{-1}). The wheat harvest showed behavior contrary to that found in other harvests, with lower yield values in the western part of the map (1800 to 2080 kg ha^{-1}); from the part located more at central part to the east of the map, the values were higher, especially for the northern region, which obtained regions above 3000 kg ha^{-1}. When analyzing the yield maps of area 2 (Figure 5), it was verified that in the soybean 2018/2019 harvest, a large part south of the map presented the lowest values for this harvest, between 1600 and 1960 kg ha^{-1}, with higher values in the northwest region, which reached yields above 2000 kg ha^{-1}.

For maize harvest (2019), the highest values were in the southeastern region of the map, between 7380 and 7500 kg ha^{-1}. For soybean 2019/2020, a large part of the map presented similar values, except for the northwest and southeast regions, with lower yields (2100 to 2420 kg ha^{-1}). The wheat crop, more to the southern part of the map, mainly in the southeast (2500 to 2700 kg ha^{-1}), presented higher yield values, in contrast, the northwest region presented the lowest yield values, between 1700 and 1900 kg ha^{-1}.

In area 1, the soybean 2018/2019 harvest obtained an average yield of 3094 kg ha^{-1} and the maize 2019 harvest, 6456 kg ha^{-1}; soybean 2019/2020 obtained an average of 3719 kg ha^{-1} and wheat 2020 reached 2511 kg ha^{-1} (Table 3). For area 2, all the harvests presented values lower than area 1, except for the maize harvest (2019), which obtained an average of 7166 kg ha^{-1} surpassing area 1 in 710 kg ha^{-1}.

Table 3: Descriptive yields statistics of areas 1 and 2

	Harvests	Means	Median	SD	Minimum	Maximum	VC
area 1	Soybean 2018/2019	3094	3068	92	2956	3253	3
	Mayze 2019	6456	6567	470	5554	7140	7
	Soybean 2019/2020	3719	3697	349	3048	4523	9
	Wheat 2020	2511	2609	327	1847	3112	13
area 2	Soybean 2018/2019	2005	1964	162	1654	2496	8
	Mayze 2019	7166	7124	170	6924	7465	2
	Soybean 2019/2020	2582	2622	162	2184	2853	6
	Wheat 2020	2232	2225	227	1787	2621	10

Subtitles: SD = Standard Deviation; VC = Coefficient of variation (%).

Figure 4: Yield maps of the four harvests in area 1.

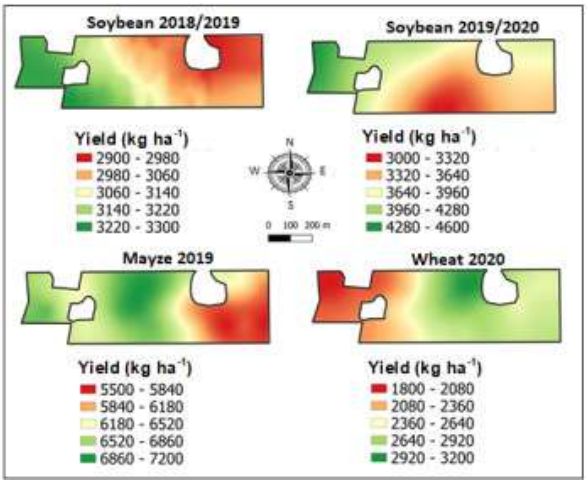

Figure 5: Yield maps of the four harvests in area 2.

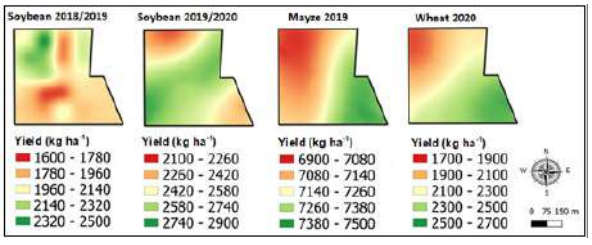

By comparing the average data of the area with those of CONAB (2021), it was observed that, for the 2018/2019 harvest, the yields of the two areas were below the national average (3337 kg ha^{-1}). According to CONAB (2019), there was a 5.5% decrease in yield in Brazil compared to the 2017-2018 harvest. In the state of Paraná, the reduction was even higher (14.8%), with 2989 kg ha^{-1}, compared to 3508 kg ha^{-1} of the previous harvest. Periods of long drought in some regions of the state, possibly influenced the occurrence of this difference. This fact may be related to the fact that the amount of rainfall in the months of November and December was lower, compared to the historical average of the property, with 121 mm (November) and 60 mm (December), totaling 181 mm. Studying the temporal variability of grain yield (soybean, maize and wheat) in property in Rio Grande do Sul over six years, Amado *et al*. (2007) observed that in normal rainfall harvests, there was a tendency for greater homogeneity among productive data, but in periods with water restriction, the difference in productivity was greater.

Whereas for soybean 2019/2020 harvest, the value of area 1 (Table 3) was higher and that of area 2 (Table 3) was lower than the national average, which was 3379 kg ha^{-1} (CONAB, 2021). In this harvest, there was a delay in sowing due to the drought, especially in the month of September (8 mm), with more expressive rains only in the second half of October, period when the areas sowing was carried out. In November, the accumulated volume was 157 mm and, mainly, in December, the volume was more expressive (277 mm).

When comparing the maize 2019 harvest, the average of the two areas was higher than the 5456 kg ha^{-1}, the Brazilian average of the second harvest. During this harvest, all months presented regular rainfall, with a highlight of 258 mm in the month of January, which possibly contributes to good germination and establishment of the crop. With 2928 kg ha^{-1} of yield average, the wheat 2020 harvest was higher than that found in this study, 2511 kg ha^{-1} (area 1) and 2232 kg ha^{-1} (area 2). The rainfall regime during the period that the crop was in the field was irregular, and on May 22nd and 23rd of 2020, there were rainfall of 133 and 83 mm, respectively, which were elevated and caused losses of soil and seed in part of the area, reflecting on final yields. In the subsequent months, there was a low rainfall rate, 61 mm (June) and 27 mm (July), returning to more expressive values only in August (150 mm).

Table 4: Spearman correlation matrix between yield data and vegetation indices for areas 1 and 2, soybean 2018/2019, maize 2019, soybean 2019/2020 and wheat 2020.

		area 1					area 2			
Soybean 2018/2019										
	VI	**PROD**	**MPRI**	**VARI**	**GLI**		**PROD**	**MPRI**	**VARI**	**GLI**
48 DAS	MPRI	-0.43*	-			60 DAS	-0.14	-		
	VARI	-0.51*	0.94*	-			-0.09	0.88*	-	
	GLI	0.01	-0.03	0.24	-		-0.09	0.37	-0.01	-
	ExG	0.01	-0.03	0.24	1.00*		-0.09	0.37	-0.01	1.00*
59 DAS	MPRI	-0.38*	-			71 DAS	0.14	-		
	VARI	-0.40*	0.99*	-			0.20	0.99*	-	
	GLI	-0.10	0.60*	0.54*	-		-0.24	-0.01	-0.11	-
	ExG	-0.10	0.59*	0.54*	1.00*		-0.24	-0.01	-0.11	1.00*
82 DAS	MPRI	0.14	-			94 DAS	0.47*	-		
	VARI	0.12	0.99*	-			0.53*	0.94*	-	
	GLI	0.19	0.16	0.13	-		0.72*	0.79*	0.91*	-
	ExG	0.19	0.15	0.13	1.00*		0.72*	0.79*	0.91*	1.00*
Mayze 2019										
30 DAS	MPRI	0.02	-			44 DAS	-0.24	-		
	VARI	0.03	0.99*	-			-0.25	0.99*	-	
	GLI	0.01	0.85*	0.88*	-		-0.03	0.83*	0.83*	-
	ExG	0.01	0.85*	0.85*	1.00*		-0.03	0.83*	0.83*	1.00*
119 DAS	MPRI	0.18	-			133 DAS	0.26	-		
	VARI	0.20	0.98*	-			-0.01	0.66*	-	
	GLI	0.26	0.16	0.28	-		-0.20	-0.25	0.45*	-
	ExG	0.26	0.15	0.27	1.00*		-0.20	-0.25	0.46*	1.00*
Soybean 2019/2020										
48 DAS	MPRI	-0.17	-			47 DAS	0.25	-		
	VARI	-0.16	0.93*	-			0.32	0.96*	-	
	GLI	-0.16	0.93*	0.88*	-		0.22	0.96*	0.88*	-
	ExG	-0.15	0.93*	0.86*	1.00*		0.22	0.96*	0.89*	1.00*
75 DAS	MPRI	0.34*	-			74 DAS	0.28	-		
	VARI	0.33*	0.99*	-			0.26	0.98*	-	
	GLI	-0.44*	-0.42*	-0.45*	-		0.15	0.88*	0.83*	-
	ExG	-0.44*	-0.41*	-0.44*	1.00*		0.15	0.88*	0.83*	1.00*
82 DAS	MPRI	-0.08	-			81 DAS	-0.07	-		
	VARI	-0.18	0.95*	-			-0.06	0.94*	-	
	GLI	0.09	0.68*	0.50*	-		-0.06	0.88*	0.74*	-
	ExG	0.09	0.68*	0.48*	1.00*		-0.06	0.88*	0.75*	1.00*
Wheat 2020										
42 DAS	MPRI	0.24	-			42 DAS	-0.28	-		
	VARI	0.14	0.90*	-			-0.29	0.99*	-	
	GLI	0.31	0.18	-0.19	-		0.21	0.18	0.15	-
	ExG	0.32	0.18	-0.19	1.00*		0.21	0.18	0.15	1.00*
65 DAS	MPRI	0.02	-			65 DAS	-0.08	-		
	VARI	-0.17	0.76*	-			-0.16	0.83*	-	
	GLI	0.19	-0.16	-0.72*	-		0.29	0.08	-0.31	-
	ExG	0.19	-0.16	-0.72*	1.00*		0.29	0.08	-0.31	1.00*
92 DAS	MPRI	0.00	-			92 DAS	-0.25	-		
	VARI	0.08	0.97*	-			-0.21	0.99*	-	
	GLI	0.24	-0.35*	-0.17	-		0.01	0.21	0.22	-
	ExG	0.23	-0.36*	-0.18	1.00*		0.01	0.21	0.22	1.00*

Subtitle: PROD = Yield. DAS = Days after sowing. Note: *Significant (p-value <0.05).

Gomes (2009) classifies CVS of all harvests as low (below 10%), except for the wheat harvest, classified as medium for both areas (Table 4).

3.3 Correlations between the vegetation indices and harvests yields and areas

By analyzing the correlations among the VIs for the two study areas, it is verified that MPRI and VARI presented, in most dates, correlations (from strong to very strong), as well as the GLI and ExG indexes, which presented correlations classified as very strong for all dates (Table 4).

Upon evaluating the correlations between VIs and crop yields for area 1, there were significant correlations between yield and MPRI (0.34) and yield and VARI (0.33), with 75 DAS in the soybean 2019/2020 harvest, classified as weak. For the other harvests, the correlations were not significant.

In area 2 (Table 4), significant correlations were found between yield and IVs, for MPRI (0.43) and VARI (0.51), with 94 DAS in 2018/2019 soybean harvest, classified as moderate correlations; GLI and ExG with 0.72, is classified as strong correlation. No significant correlations were found in the remaining harvests.

By evaluating the correlation between VARI and soybean yield, using an eBee model PPA with RGB camera, Prestes *et al*. (2020) verified correlations with r values between 0.8 (96 DAS) and 0.64 (121 DAS), which were higher than those found in the present study. Monteiro (2021), evaluating the temporal spectrum behavior of soybeans through vegetation indices, found that soybean productivity showed a moderate correlation (r = 0.45) with VARI.

Comparing MPRI and yield in different stages of soybean crops in an experiment in the municipality of Londrina - PR, Franchini *et al*. (2018) found positive correlations in four moments evaluated throughout the culture cycle, with values of 0.49, 0.54, 0.37 and 0.29, respectively. Sanches *et al*. (2018), in an experiment carried out in Itirapina - SP, obtained significant correlations of 0.83 when evaluating sugarcane yield and MPRI index.

By correlating soybean yield with vegetation indices of the visible length, namely: MPRI, VARI, ExG and GLI, on six flights performed with RPA, using RGB camera, Silva (2020) found that the correlations varied between very weak and moderate, with r of a maximum of 0.50. Whereas for wheat crop, the correlations were from 0.24 to 0.49, being higher for the GLI and MPRI indices. García-Martínez *et al*. (2020), in work on estimating corn grain yield from vegetation indices, found at 79 DAS a correlation between productivity and ExG of 0.71 and between productivity and VARI (0.67). Luna Neto *et al*. (2023), evaluating the correlation of corn crops subjected to biostimulants, found a correlation between EXG and productivity of 0.02. Upon evaluating crop wheat in Spain, Fernandez-Gallego *et al*. (2019) observed that the highest correlations of the RGB indices (among them the MPRI) with the wheat grains yield were observed when the canopy color began to change from green to yellow.

In a study by Albert (2020), using MPRI in maize, a significant positive correlation of 0.67 was found in stage V6. Whereas in V9, it was negative, having significance.

Gutierrez *et al*. (2012) demonstrated that the use of VIs in the yield estimate may have restrictions in some situations, especially when there is an imbalance between the stages of crop development, which may be affected by some stress suffered by the plant. Vianna (2020), evaluating different IVs in soybean genetic improvement, found correlations in phase R.5, between soybean productivity and the GLI index, ranging from 0.26 to 0.58, and between soybean productivity and VARI, between 0.42 and 0.78.

In general, for all the harvests analyzed, there were many variabilities related to the correlations between the VIs and yield. Venteris *et al*. (2015) reported that temporal analyzes of VIs data with agricultural crops yields may be impaired due to the interference of several factors, among which the differences in the date of image acquisition and the interaction with the crop growth stage can be highlighted. It is worth pointing out that due to climatic factors, a larger number of flights could not be carried out, which might reflect in some period that would better express the existing relationships among the studied variables.

4 CONCLUSIONS

According to the research, it is suggested that the farmer carry out surveys with RPA with RGB camera in soybean crop, mainly in R7 stage, in maize at VT (bolting) stage and in wheat at tillering stage, since these phenological stages showed higher correlations and between the VIs and the yield of each crop.

The pairs of VIs MPRI and VARI, GLI and ExG were similar as vegetative indicators, so only two of them would already have the capacity to represent the variations existing in the areas of the study between the dates.

REFERENCES

ALBERT, A. M. **Índices de vegetação obtidos com**

câmera multiespectral relacionados com adubação nitrogenada e produtividade no milho. Dissertação (Trabalho de Conclusão do Curso (Graduação em Agronomia)) — Instituto Federal de Educação, Ciência e Tecnologia Goiano, Rio Verde, 2020. 35f.

ALEXOPOULOS, A.; KOUTRAS, K.; ALI, S. B.; PUCCIO, S.; CARELLA, A.; OTTAVIANO, R.; KALOGERAS, A. Complementary use of ground-based proximal sensing and airborne/spaceborne remote sensing techniques in precision agriculture: A systematic review. **Agronomy**, MDPI, v. 13, n. 7, p. 1942, 2023.

AMADO, T. J. C.; PONTELLI, C. B.; SANTI, A. L.; VIANA, J. H. M.; SULZBACH, L. A. d. S. **Variabilidade espacial e temporal da produtividade de culturas sob sistema plantio direto**. Pesquisa Agropecuária Brasileira, SciELO Brasil, v. 42, n. 8, p. 1101–1110, 2007.

Andrade Junior, A. S. d.; MELO, F. d. B.; BASTOS, E. A.; CARDOSO, M. J. **Evaluation of the nutritional status of corn by vegetation indices via aerial images**. Ciência Rural, SciELO Brasil, v. 51, n. 8, p. e20200692, 2021.

APARECIDO, L. E. d. O.; ROLIM, G. d. S.; RICHETTI, J.; SOUZA, P. S. d.; JOHANN, J. A. **Köppen, Thornthwaite and Camargo climate classifications for climatic zoning in the State of Paraná, Brazil**. Ciência e Agrotecnologia, SciELO Brasil, v. 40, n. 4, p. 405–417, 2016.

BALLESTEROS, R.; ORTEGA, J. F.; HERNANDEZ, D.; CAMPO, A. D.; MORENO, M. A. Combined use of agro-climatic and very high-resolution remote sensing information for crop monitoring. **International journal of applied earth observation and geoinformation**, Elsevier, v. 72, n. 1, p. 66–75, 2018.

BANERJEE, B. P.; RAVAL, S. A.; CULLEN, P. J. Alignment of uav-hyperspectral bands using keypoint descriptors in a spectrally complex environment. **Remote sensing letters**, Taylor & Francis, v. 9, n. 6, p. 524–533, 2018.

BARBEDO, J. G. A. A review on the use of unmanned aerial vehicles and imaging sensors for monitoring and assessing plant stresses. **Drone**, MDPI, v. 3, n. 2, p. 40, 2019.

BRASIL. Ministério da Agricultura, Pecuária e Abastecimento. Secretaria de Defesa Agropecuária. **Regras para análise de sementes.** Brasília: Mapa/ACS, 2009.

CALLEGARI-JACQUES, S. M. **Bioestatística: princípios e aplicações.** 1. ed. Porto Alegre: Artmed, 2003.

CONAB. **Acompanhamento da safra brasileira.** Grãos. Décimo segundo levantamento, Setembro 2019. Safra 2018/2019. Brasília, DF: CONAB, 2019. V. 6. p.1-47. 2019. Disponível em: https://www.conab.gov.br/info-agro/safras/graos/boletim-da-safra-de-graos. Acesso em: 02 out. 2019.

CONAB. **Acompanhamento da safra brasileira.** Grãos. Sétimo levantamento. Safra 2020/2021. Brasília, DF: CONAB. 2021. Disponível em: https://www.conab.gov.br/info-agro/safras/graos/boletim-da-safra-de-graos. Acesso em: 15 mar. 2021.

COSTA, L.; NUNES, L.; AMPATZIDIS, Y. A new visible band index (vndvi) for estimating ndvi values on rgb images utilizing genetic algorithms. **Computers and Electronics in Agriculture**, Elsevier, v. 172, n. 1, p. 105334, 2020.

EMBRAPA. Centro Nacional de Pesquisa de Solos. **Sistema brasileiro de classificação de solos.** 5. ed. Rio de Janeiro: Embrapa, 2018.

FERNANDEZ-GALLEGO, J. A.; KEFAUVER, S. C.; VATTER, T.; GUTIÉRREZ, N. A.; NIETO-TALADRIZ, M. T.; ARAUS, J. L. Low-cost assessment of grain yield in durum wheat using rgb images. **European Journal of Agronomy**, v. 105, n. 1, p. 146–156, 2019.

FRANCHINI, J.; JUNIOR, A. A. B.; JORGE, L. D. C.; DEBIASI, H.; DIAS, W.; GODOY, C.; OLIVEIRA, M. C. N. **Uso de imagens aéreas obtidas com drones em sistemas de produção de soja**. Londrina: Embrapa Soja, 2018.

FREIRE-SILVA, J.; PAZ, Y. M.; LIMA-SILVA, P. P.; PEREIRA, J. D.; CANDEIAS, A. L. B. Remote sensing vegetation index for processing images in the visible band (rgb). **Journal of Hyperspectral Remote Sensing**, v. 9, n. 4, p. 228–239, 2019.

GARCÍA-MARTÍNEZ, H.; FLORES-MAGDALENO, H.; ASCENCIO-HERNÁNDEZ, R.; KHALIL-GARDEZI, A.; TIJERINA-CHÁVEZ, L.; MANCILLA-VILLA, O. R.; VÁZQUEZ-PEÑA, M. A. Corn grain yield estimation from vegetation

indices, canopy cover, plant density, and a neural network using multispectral and rgb images acquired with unmanned aerial vehicles. **Agriculture (Switzerland)**, v. 10, n. 7, p. 1–24, 2020.

GITELSON, A. A.; VIÑA, A.; ARKEBAUER, T. J.; RUNDQUIST, D. C.; KEYDAN, G.; LEAVITT, B. **Remote estimation of leaf area index and green leaf biomass in maize canopies**. Geophysical research letters, Wiley Online Library, v. 30, n. 5, p. 52(1–4), 2003.

GOMES, F. P. **Curso de estatística experimental.** 15. Ed, FEALQ. 2009. 451 p.

GUTIERREZ, M.; NORTON, R.; THORP, K. R.; WANG, G. Association of spectral reflectance indices with plant growth and lint yield in upland cotton. **Crop Science**, Wiley Online Library, v. 52, n. 2, p. 849–857, 2012.

HOYOS-VILLEGAS, V.; FRITSCHI, F. Relationships among vegetation indices derived from aerial photographs and soybean growth and yield. **Crop Science**, Wiley Online Library, v. 53, n. 6, p. 2631–2642, 2013.

HUETE, A. R. A soil-adjusted vegetation index (savi). **Remote sensing of environment**, Elsevier, v. 25, n. 3, p. 295–309, 1988.

INMAN, H. F. Karl pearson and ra fisher on statistical tests: a 1935 exchange from nature. **The American Statistician**, Taylor & Francis, v. 48, n. 1, p. 2–11, 1994.

LOUHAICHI, M.; BORMAN, M. M.; JOHNSON, D. E. Spatially located platform and aerial photography for documentation of grazing impacts on wheat. **Geocarto International**, Taylor & Francis, v. 16, n. 1, p. 65–70, 2001.

Luna Neto, E. V.; SILVA, A. V. da; SILVA, J. H. B. da; SILVA, C. M. da; COSTA, T. R. S.; MIELEZRSKI, F. Índices espectrais de vegetação no monitoramento do milho (*Zea mays L.*) submetidos à bioestimulantes. **Nativa**, v. 11, n. 3, p. 323–330, 2023.

MINITAB. **Minitab for Windows**. Xx. USA: State College Statistical Software, 2003.

MONTEIRO, P. H. S. **Comportamento espectro-temporal da soja utilizando sensores orbitais e não orbital e correlação dos índices de vegetação com a produtividade.** Dissertação (Mestrado em Agronomia) — Universidade Tecnológica Federal do Paraná, Pato Branco, Pato Branco, 2021.

PRESTES, C. D. P.; GUIMARÃES, A. M.; ZAMPIER, D. P.; GABARDO, G.; CAIRES, E. F.; ASATO, B. R. Avaliação de metodologia de estimativa de produtividade de soja por meio de aeronave não tripulada e técnica de aprendizado de máquina baseada em regressão. **Revista Mundi Engenharia, Tecnologia e Gestão**, v. 5, n. 3, p. 254 (01–12), 2020.

QGIS. **Sistema de Informação Geográfica.** Project! Qgis. 2021. Disponível em: http://www.qgis.org/. Acesso em: 25 mar. 2021.

ROUSE, J. W.; HAAS, R. H.; SCHELL, J. A.; DEERING, D. W. **Monitoring vegetation systems in the Great Plains with ERTS**. *In*: Earth Resources Technology Satellite Symposium. Washington: NASA Spec. Publ, 1974. (3, 1), p. 309–317.

SANCHES, G. M.; DUFT, D. G.; KÖLLN, O. T.; LUCIANO, A. C. d. S.; CASTRO, S. G. Q. D.; OKUNO, F. M.; FRANCO, H. C. J. The potential for rgb images obtained using unmanned aerial vehicle to assess and predict yield in sugarcane fields. **International Journal of Remote Sensing**, Taylor & Francis, v. 39, n. 15-16, p. 5402–5414, 2018.

SEMERARO, T.; MASTROLEO, G.; POMES, A.; LUVISI, A.; GISSI, E.; ARETANO, R. Modelling fuzzy combination of remote sensing vegetation index for durum wheat crop analysis. **Computers and Electronics in Agriculture**, Elsevier, v. 156, n. 1, p. 684–692, 2019.

SILVA, L. C. A. **Delineamento de zonas de manejo por imagens suborbitais, orbitais e variáveis de solo**. Dissertação (Mestrado em Engenharia Agrícola) — Universidade Estadual do Oeste do Paraná, Cascavel, 2020.

VENTERIS, E. R.; TAGESTAD, J.; DOWNS, J.; MURRAY, C. Detection of anomalous crop condition and soil variability mapping using a 26 year landsat record and the palmer crop moisture index. **International Journal of Applied Sarth Observation and Geoinformation**, Elsevier, v. 39, n. 1, p. 160–170, 2015.

VIANNA, M. S. **Evaluation of vegetation indices from aerial images in soybean breeding.** Dissertação (Mestrado) — Escola superior de Agricultura "Luíz de Queiroz", Piracicaba, 2020.

WEISS, M.; JACOB, F.; DUVEILLER, G. Remote sensing for agricultural applications: A meta-review. **Remote Sensing of Environment**, Elsevier, v. 236, n. 1, p. 111402, 2020.

WOEBBECKE, D. M.; MEYER, G. E.; BARGEN, K. V.; MORTENSEN, D. A. **Color indices for weed identification under various soil, residue, and lighting conditions**. Transactions of the ASAE, American Society of Agricultural and Biological Engineers, v. 38, n. 1, p. 259–269, 1995.

YANG, Z.; WILLIS, P.; MUELLER, R. **Impact of band-ratio enhanced AWIFS image to crop classification accuracy**. *In*: Proc. Pecora. Colorado: Maryland, 2008. v. 17, n. 1, p. 1–11.

YUZUGULLU, O.; LORENZ, F.; FRÖHLICH, P.; LIEBISCH, F. Understanding fields by remote sensing: Soil zoning and property mapping. **Remote Sensing**, MDPI, v. 12, n. 7, p. 1116, 2020.

ZHOU, M.; MA, X.; WANG, K.; CHENG, T.; TIAN, Y.; WANG, J.; ZHU, Y.; HU, Y.; NIU, Q.; GUI, L. *et al*. Detection of phenology using an improved shape model on time-series vegetation index in wheat. **Computers and electronics in agriculture**, Elsevier, v. 173, n. 1, p. 105398, 2020.